Modeling and Stability Analysis of Automatic Generation Control Over Cognitive Radio Networks in Smart Grids

Shichao Liu, Peter X. Liu, *Senior Member, IEEE,* and Abdulmotaleb El Saddik, *Fellow, IEEE*

***Abstract*—Due to its great potential to improve the overall performance of data transmission with its dynamic and adaptive spectrum allocation capability in comparison with many other networking technologies, cognitive radio (CR) networking technology has been increasingly employed in networking and communication infrastructures for smart grids. However, a secondary user (SU) of a CR network has to be squeezed out from a channel when a primary user reclaims the channel, which may occur in a randomized fashion. The random interruption of SU traffic may cause packet losses and delays for SU data, and it will in turn affect the stability of the monitoring and control of smart grids. In this paper, we address this problem and investigate the modeling and stability analysis of the automatic generation control (AGC) of a smart grid for which CR networks are used as the infrastructure for the aggregation and communication of both system-wide information and local measurement data. For this purpose, a randomly switched power system model is proposed for the AGC of the smart grid. By modeling the CR network as an On–Off switch with sojourn times, the stability of the AGC of the smart grid is analyzed. In particular, we investigate the smart grid with two main types of CR networks: 1) the sojourn times are arbitrary but bounded and 2) the sojourn times follow an independent and identical distribution process. The sufficient conditions are obtained for the stability of the AGC of the smart grid with these two CR networks, respectively. Simulation results show the effects of the CR networks on the dynamic performance of the AGC of the smart grid and illustrate the usefulness of the developed sufficient conditions in the design of CR networks in order to ensure the stability of the AGC of the smart grid.**

***Index Terms*—Automatic generation control (AGC), cognitive radio (CR), modeling, smart grid, stability analysis, switched system.**

I. Introduction

A SMART grid integrates advanced two-way communication networks and intelligent computing technologies into current power systems, from large-scale generation through delivery units to electricity consumers [1], [2]. The applications of a smart grid include wide-area monitoring, control and protection (WAMCP), distributed generation management, advanced metering infrastructure (AMI), real-time pricing, etc. [3]–[5]. To support these applications, there are several unique challenges to be addressed for smart grid communications [6]–[9]. First of all, since WAMCP and AMI involve tremendous amounts of information exchange over wide geographical areas, it needs large bandwidths for both data transmission and collection. Secondly, as most of AMI communication architectures are formed among smart meters for data routing in the 2.4 GHz industrial, scientific, and medical (ISM) band, signal interferences will be severe among these types of radio systems. Last but not least, because a smart grid communication architecture consists of wide area network architecture (WAN), neighborhood area network architecture (NAN) and home area network architecture (HAN), these heterogeneous network architectures require the capability to coordinate communications within each subarea and between different areas. However, most of the traditional communication technologies are infeasible to meet all these requirements.

Due to its great potential to enhance the overall performance of data communications with its dynamic and adaptive spectrum management capabilities, the cognitive radio (CR) network has been increasingly considered as the networking and communication infrastructure for smart grids [8]–[10]. In view of the fact that a large portion of the licensed radio spectrum remains severely under-utilized, the CR technology is proposed to achieve the efficient usage of the assigned radio spectrum [11]–[14]. In a CR network, there are two kinds of users. Primary users (PUs) are the users who are licensed with certain bands of the current spectrum, while secondary users (SUs) do not have the licenses for the utilization of those spectrum bands. However, SUs can opportunistically sense and identify the unused channels in the licensed spectrum. Based on the sensed results, SUs are able to use the available channels, coordinate the spectrum access with other users, and return the channel back to PUs when PUs reclaim the spectrum. With the capability of the dynamic and opportunistic spectrum allocation, CR networks can increase spectrum efficiency, enable different large-scale spectrum regulations, and coordinate radio spectrum sharing among different area networks in smart grids.

Although CR networks have great potential to address the unique challenges for smart grid communications in

Manuscript received August 20, 2013; revised March 22, 2014; accepted June 16, 2014. Date of publication September 12, 2014; date of current version January 13, 2015. This work was supported in part by the Natural Sciences and Engineering Research Council of Canada and in part by the Carleton President 2010 Ph.D. Fellowship. This paper was recommended by Associate Editor N. N. Xiong.

S. Liu and P. X. Liu are with the Department of Systems and Computer Engineering, Carleton University, Ottawa, ON K1S 5B6, Canada (e-mail: lshchao@sce.carleton.ca; xpliu@sce.carleton.ca).

A. El Saddik is with the School of Information Technology and Engineering, University of Ottawa, Ottawa, ON K1N 6N5, Canada (e-mail: abed@mcrlab.uottawa.ca).

Color versions of one or more of the figures in this paper are available online at http://ieeexplore.ieee.org.

Digital Object Identifier 10.1109/TSMC.2014.2351372

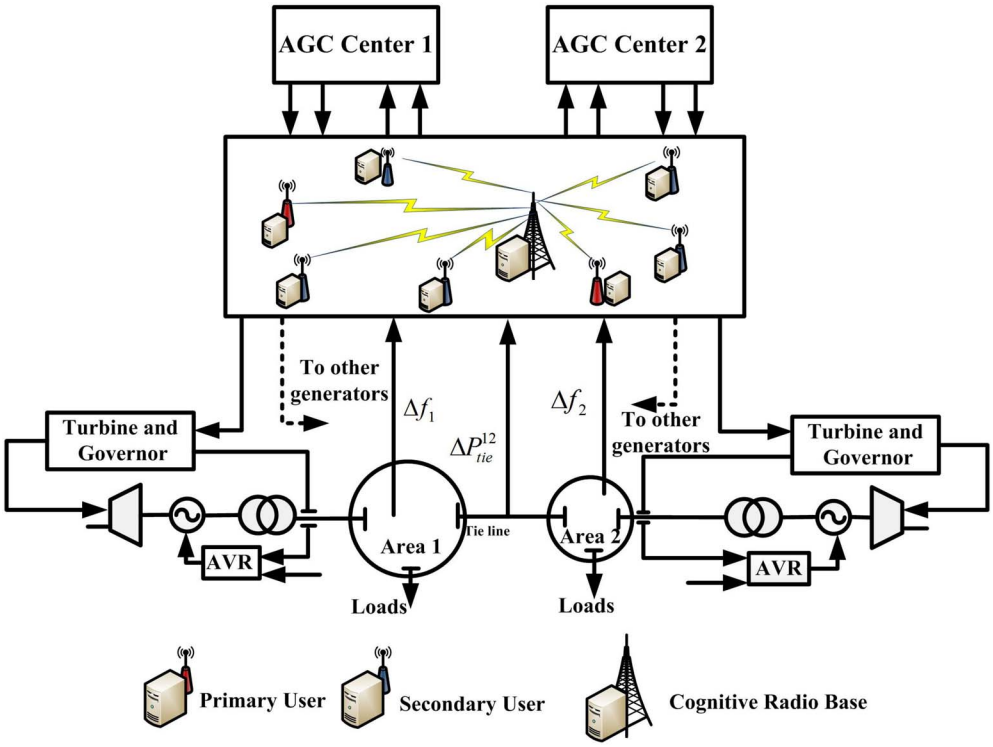

Fig. 1. Two-area power system over CR networks.

comparison with many other networking technologies, they bring in a new problem. Specifically, a SU of a CR network has to be squeezed out from the channel that it is using when a PU reclaims the channel, this may occur in a randomized fashion. The random interruption of SU traffic will unavoidably cause packet loss for SU data. The lost data packet can be of any nature: control commands from control centers to substations, sensed data from remote terminal units (RTUs), real-time pricing information between utilities and customers, etc. The loss of data packets may lead to very severe and adverse effects on the management and control of a smart grid. In [15], it is emphasized that communication failures in a power grid may cause very serious problems for both system operation and control. In [16], it is noticed that communication failures can interrupt the wide area damping control of power systems. In [17], it is found that communication topology changes among distributed damping controllers can jeopardize the power system performance. In [18] and [19], it is reported that the reliability of the cooperative control of distributed energy resources (DERs) in distribution networks can be degraded by communication failures in communication channels. In [20], the dynamic performance of the automatic generation control (AGC) of a four-area power system is found to greatly depend on communication topologies among local-area controllers.

Therefore, it is very important to deal with the above problem and to understand the effects of the random interruption of SU traffic in CR networks on the stability and performance of the smart grid operation and control. In [21] and [22], the state estimation of networked systems over CR networks and its application in smart grids are studied. By modeling the CR network as a semi-Markov process, the stability of a linear quadratic Gaussain (LQG) estimator is investigated. However, the effect of a CR network on the smart grid control, such as AGC, is not covered in these work.

In this paper, we investigate the modeling and stability analysis of the AGC of a smart grid for which CR networks are used as the infrastructure for the aggregation and communication of both system-wide information and local measurement data. The contributions of this paper can be summarized as follows.

1) By modeling CR networks as On–Off switches with sojourn times, a novel switched power system model is proposed for the AGC of the smart grid.
2) The stability of the AGC of the smart grid is analyzed. We investigate the smart grid with two main types of CR networks: a) the sojourn time is arbitrary but bounded and b) the sojourn time follows an independent and identical distribution (IID) process. Sufficient conditions are obtained for the stability of the AGC of the smart grid with these two CR networks, respectively. Simulation studies show that the obtained results are very useful to the design of CR networks in order to guarantee the stochastic stability of the AGC of the smart grid.

The remainder of this paper is organized as follows. In Section II, a new switched system model is proposed to investigate the effects of CR networks on the stability of the AGC of a smart grid. The stability of the AGC of the smart grid over CR networks is studied for both deterministic and stochastic sojourn time situations in Section III. In

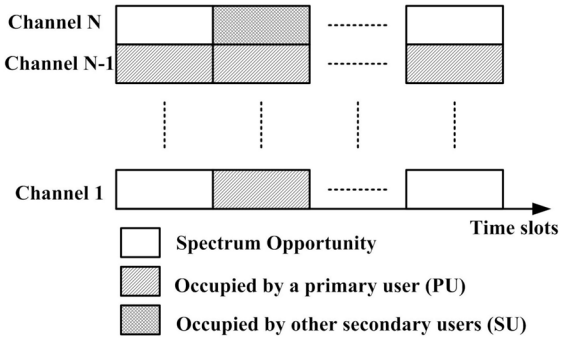

Fig. 2. CR channel illustration.

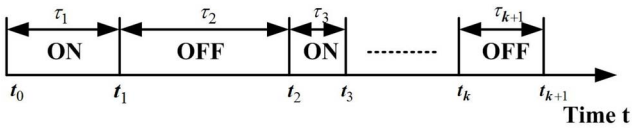

Fig. 3. Proposed On–Off cognitive channel model.

Section IV, a two-area power system is used for performance analysis. Finally, Section V concludes the paper and describes future work.

Notation: The superscript "T" denotes the transposition of vectors or matrix. Notation $P > 0$ means positive definite.

II. Modeling of Automatic Generation Control in Interconnected Power Systems Over CR Networks

The AGC over CR networks in a smart grid is shown in Fig. 1. In this AGC, there are two loops of data transmissions. One is the feed-forward loop in which control centers send control signals to RTUs. The other one is the feedback loop where measurement signals are transmitted from RTUs to the control centers over the CR wireless network. It can been noticed that the AGC is a typical networked control system (NCS) [23]–[26], a cyber-physical energy system [27], [28], or a special system in [29].

In this section, a new On–Off switch model of the CR network in the smart grid is proposed. By using this On–Off switch model, a randomly switched linear system is proposed to integrate the dynamic of the CR network in the cyber layer into the physical power system in the smart grid.

A. Model of the CR Network

As shown in Fig. 2, we consider a licensed spectrum band consisting of N nonoverlapping channels in the CR network used by the smart grid. Both PUs and SUs in this radio network are operated synchronously in a time-slotted fashion. We consider the situation in which each cognitive user can sense only one channel at each time slot. The availability of each channel is modeled as a 2-state Markov chain (MC) in [12]–[14]. However, in terms of the system performance of a smart grid, we should take account of not only the state transitions, but also the time staying in each state. From each SU point of view, the sensed channel state is either free or occupied by other users. This means the communication channel for data exchange is either ON or OFF. Thus, we model the communication channel as an ON–OFF switch with sojourn times, shown in Fig. 3. A sojourn time τ_i is a time interval the communication channel continuously stays in a state, either ON or OFF [30]. Let the channel state at kth time instant denoted by $\theta_k \in \Theta = \{0, 1\}$, where $\Theta = \{0, 1\}$ is the state space of θ_k, 0 denoting OFF state of the channel, 1 denoting ON state.

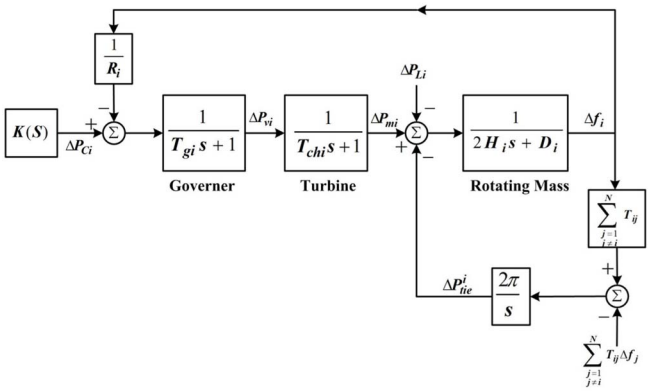

Fig. 4. Block diagram of the control area i.

B. Switched System Model for Automatic Generation Control in Smart Grids

An AGC system is in charge of the operation of the frequency control in a power system [31]. It mainly keeps the frequency of the power system at a nominal value (i.e., 60 Hz) by adjusting power generation set points. For the AGC of a largely interconnected power system, the power system is decomposed into several control areas which are interconnected by high-voltage tie lines. In each control area, it comprises a group of generators and a number of loads. Commonly, the generators in each area are represented equivalently by one single machine and the loads by one single load. Furthermore, although power systems are usually nonlinear, linearized models are used because the AGC operation only involves relatively small disturbances [32], [33].

The control structure of an equivalent linearized model in the ith control area is shown in Fig. 4. A nonreheat steam turbine is considered. When the governor senses the frequency changes Δf_i, it adjusts the valve position ΔP_{v_i}. By doing this, the input of steam flowing into the turbine is regulated and thus the mechanical power ΔP_{m_i} is controlled. As a result, the frequency is kept constant. The governor and turbine compose the primary frequency control of this generating unit. However, the system frequency is usually not able to be restored to the nominal value (i.e., 60 Hz) by only using the primary control. A secondary frequency controller $K(s)$ is necessary to adjust the load reference set point ΔP_{c_i} for the turbine to make the power generation ΔP_{m_i} track the load changes ΔP_{L_i} and restore the system frequency.

The turbine dynamic is described by

$$\Delta \dot{P}_{m_i} = -\frac{1}{T_{ch_i}} \Delta P_{m_i} + \frac{1}{T_{\mathrm{ch}_i}} \Delta P_{v_i} \tag{1}$$

where, ΔP_{m_i} is the generator mechanical power deviation, ΔP_{v_i} is turbine valve position deviation, and T_{ch_i} is the time constant of turbine i.

The governor dynamic is described by

$$\Delta \dot{P}_{v_i} = -\frac{1}{R_i T_{g_i}} \Delta f_i - \frac{1}{T_{g_i}} \Delta P_{v_i} + \frac{1}{T_{g_i}} \Delta P_{c_i} \tag{2}$$

where, Δf_i is the frequency deviation of area i, ΔP_{c_i} is the load reference set-point, T_{g_i} is the time constant of governor i, and R_i is the speed droop coefficient.

The overall load-generation dynamic is described by

$$\Delta \dot{f}_i = -\frac{D_i}{2H_i} \Delta f_i + \frac{1}{2H_i} \Delta P_{m_i} - \frac{1}{2H_i} \Delta P^i_{\text{tie}} - \frac{1}{2H_i} \Delta P_{L_i} \tag{3}$$

where, ΔP^i_{tie} is the net tie-line power flow in area i, ΔP_{L_i} is the load deviation, H_i is the equivalent inertia constant of area i, and D_i is the equivalent damping coefficient of area i.

The dynamic of the net tie-line power flow dynamic is

$$\Delta \dot{P}^i_{\text{tie}} = \sum_{j=1, j\neq i}^{N} 2\pi T_{ij} \left(\Delta f_i - \Delta f_j \right) \tag{4}$$

where T_{ij} is the synchronizing power coefficient, and Δf_j is the frequency deviation of area j.

Furthermore, we assume there are N interconnected areas in the power system. We can write the state-space model of the above dynamics for AGC in area i as follows:

$$\dot{x}_i = A_{ii} x_i + B_i u_i + \sum_{j=1, j\neq i}^{N} A_{ij} x_j + F_i \Delta P_{L_i}, x_i(0) = x_0 \tag{5}$$

where

$$x_i = \begin{bmatrix} \Delta f_i & \Delta P_{m_i} & \Delta P_{v_i} & \Delta P^{ij}_{\text{tie}} \end{bmatrix}^T; u_i = \Delta P_{c_i}$$

$$A_{ii} = \begin{bmatrix} -\frac{D_i}{2H_i} & \frac{1}{2H_i} & 0 & -\frac{1}{2H_i} \\ 0 & -\frac{1}{T_{\text{ch}_i}} & \frac{1}{T_{\text{ch}_i}} & 0 \\ -\frac{1}{R_i T_{g_i}} & 0 & -\frac{1}{T_{g_i}} & 0 \\ \sum_{j=1, j\neq i}^{N} 2\pi T_{ij} & 0 & 0 & 0 \end{bmatrix}$$

$$A_{ij} = \begin{bmatrix} 0 & 0 & 0 & 0 \\ 0 & 0 & 0 & 0 \\ 0 & 0 & 0 & 0 \\ -2\pi T_{ij} & 0 & 0 & 0 \end{bmatrix}$$

$$B_i = \begin{bmatrix} 0 & 0 & \frac{1}{T_{g_i}} & 0 \end{bmatrix}^T; F_i = \begin{bmatrix} -\frac{1}{M_i} & 0 & 0 & 0 \end{bmatrix}^T.$$

For the whole multiarea power system, a linear time-invariant (LTI) interconnected model is given by

$$\dot{\mathbf{x}} = \mathbf{A_c x} + \mathbf{B_c u} + \mathbf{F} \Delta \mathbf{P_L}, \mathbf{x}(0) = \mathbf{x}_0 \tag{6}$$

where

$$\mathbf{x} = \begin{bmatrix} x_1 & x_2 & \cdots & x_N \end{bmatrix}^T; \mathbf{u} = \begin{bmatrix} u_1 & u_2 & \cdots & u_N \end{bmatrix}^T$$

$$\Delta \mathbf{P_L} = \begin{bmatrix} \Delta P_{L1} & \Delta P_{L2} & \cdots & \Delta P_{LN} \end{bmatrix}^T$$

$$\mathbf{A_c} = \begin{bmatrix} A_{11} & A_{12} & \cdots & A_{1N} \\ A_{21} & A_{22} & \cdots & A_{2N} \\ \vdots & \vdots & \ddots & \vdots \\ A_{N1} & A_{N2} & \cdots & A_{NN} \end{bmatrix}$$

$$\mathbf{B_c} = \text{diag} \begin{Bmatrix} B_1 & B_2 & \cdots & B_N \end{Bmatrix}^T$$

$$\mathbf{F} = \text{diag} \begin{Bmatrix} F_1 & F_2 & \cdots & F_N \end{Bmatrix}^T.$$

The above state-space model can be written in a more convenient form as the steady state is denoted by $\mathbf{x}_{ss}$ [34]

$$\dot{\mathbf{x}} = \mathbf{A_c x} + \mathbf{B_c u}, \mathbf{x}(0) = -\mathbf{x}_{ss}. \tag{7}$$

The sampled discrete-time model is

$$\mathbf{x}(k+1) = \mathbf{A x}(k) + \mathbf{B u}(k) \tag{8}$$

where $\mathbf{A} = e^{\mathbf{A_c} h}$, $\mathbf{B} = \int_0^h e^{\mathbf{A_c} \tau} \mathbf{B_c} d\tau$, h is the sampling period.

The above power model is under the assumption that the communication channels between the control center and RTUs are perfect. However, as we discussed in the previous section, the fact that PUs reclaim the channel will cause packet loss when data are transferring from SUs. The channel state at the kth time slot is denoted by $\theta_k \in \Theta = \{0, 1\}$, where 0 denotes the OFF state of the channel (packets are lost), and 1 denotes the ON state (packets are received successfully). Therefore, a new switched system model is proposed for the AGC over CR networks in the smart grid. Zero-order-holds (ZOHs) are used in the control center [35]. Considering the time interval $l \in [t_k, t_{k+1})$, where t_k, t_{k+1} are two consecutive state jump instants, the state-feedback controller with its gain matrix $\mathbf{K}$ for the AGC has the following two modes:

$$u(l) = \begin{cases} \mathbf{K x}(l), \theta_{t_k} = 1 \\ \mathbf{K x}(t_k), \theta_{t_k} = 0. \end{cases} \tag{9}$$

Plugging the above state-feedback controller into the power system (8), the dynamics of the closed-loop power system can be described by the following linear switched system during the time interval $l \in [t_k, t_{k+1})$:

$$\mathbf{x}(l+1) = \begin{cases} (\mathbf{A} + \mathbf{BK})\, \mathbf{x}(l), \theta_{t_k} = 1 \\ \mathbf{A x}(l) + \mathbf{BK x}(t_k), \theta_{t_k} = 0. \end{cases} \tag{10}$$

The initial instant is denoted by t_0 and the initial state $\mathbf{x}(t_0)$ and θ_{t_0} are initial conditions. Until t_{k+1}, the sojourn time sequence is $\{\tau_1, \tau_2, \ldots, \tau_i, \ldots, \tau_{k+1}\}$, where $\tau_i = t_{i+1} - t_i$. In view of the fact that PUs opportunistically reclaim the communication channel in the CR network, the sojourn time is time-varying. Consequently, the closed-loop power system becomes a time-varying linear switched system.

III. Stability of Automatic Generation Control Over CR Networks

In the previous section, we propose a time-varying linear switched system model for the closed-loop power system over

CR networks. In this section, the stability of the AGC over CR networks in the smart grid is going to be studied and sufficient conditions will be given for both the asymptotical stability and the mean-square stability of the smart grid under different CR network situations. Here, we consider the case that sojourn time variables $\tau_i \in \{\tau_1, \tau_2, \ldots, \tau_i, \ldots, \tau_{k+1}\}$ are independent.

A. Asymptotical Stability for the Arbitrary but Bounded Sojourn Times

Definition 1: For arbitrary sojourn times $\tau_i \in [\tau_{\min}, \tau_{\max}], i \in \{0, 1, \ldots, k+1\}$, the state trajectory $\mathbf{x}(l)$ in (10) with initial conditions $\mathbf{x}(t_0) = \mathbf{x}_0$ and $\theta_{t_0} = \theta_0 \in \Theta = \{0, 1\}$ is globally asymptotically stable if for any $\epsilon > 0$, there exists a $\beta > 0$, whenever $||\mathbf{x}_0|| < \beta$, $\mathbf{x}(l)$ satisfies $||\mathbf{x}(l, t_0, \mathbf{x}_0)|| < \epsilon$ for any $l > t_0$, and $\lim_{l\to\infty} ||\mathbf{x}(l, t_0, \mathbf{x}_0)|| = 0$.

Theorem 1: The power system (10) is globally asymptotically stable for all the arbitrary sojourn times $\tau_i \in [\tau_{\min}, \tau_{\max}], i \in \{0, 1, \ldots, k+1\}$ if all the eigenvalues of the matrices $(\mathbf{A}^{\tau_i} + \sum_{r=0}^{\tau_i-1} \mathbf{A}^r\mathbf{BK})$ are inside the unity circle.

Proof: Without loss of generality, we consider the initial conditions $\mathbf{x}(t_0) = \mathbf{x}_0$ and $\theta_{t_0} = 1$ which means the communication channel is ON and packets are successfully transmitted. During the time interval $l \in [t_0, t_{k+1})$, the sojourn time sequence is $\{\tau_1, \tau_2, \ldots, \tau_i, \ldots, \tau_k, \tau_{k+1}\}$, and the corresponding state sequence is $\{1, 0, 1, 0, \ldots, 1, 0\}$. On the time interval $l \in [t_k, t_{k+1})$, $\theta_{t_k} = 0$, the system (10) has the following state response:

$$\mathbf{x}(l) = \left(\mathbf{A}^{l-t_k} + \sum_{r=0}^{l-t_k-1} \mathbf{A}^r\mathbf{BK}\right)\mathbf{x}(t_k). \tag{11}$$

Using the system (10), $\mathbf{x}(t_k)$ has the following response:

$$\mathbf{x}(t_k) = (\mathbf{A} + \mathbf{BK})^{\tau_k}\,\mathbf{x}\,(t_{k-1}). \tag{12}$$

And

$$\mathbf{x}\,(t_{k-1}) = \left(\mathbf{A}^{\tau_{k-1}} + \sum_{r=0}^{\tau_{k-1}} \mathbf{A}^r\mathbf{BK}\right)\mathbf{x}\,(t_{k-2}). \tag{13}$$

By doing this deduction, the state $\mathbf{x}(l)$ finally has the following form:

$$\begin{aligned}\mathbf{x}(l) = &\left(\mathbf{A}^{l-t_k} + \sum_{r=0}^{l-t_k-1} \mathbf{A}^r\mathbf{BK}\right) \times (\mathbf{A} + \mathbf{BK})^{\tau_k} \\ &\times \left(\mathbf{A}^{\tau_{k-1}} + \sum_{r=0}^{\tau_{k-1}} \mathbf{A}^r\mathbf{BK}\right) \times \cdots \times (\mathbf{A} + \mathbf{BK})^{\tau_1}\,\mathbf{x}_0.\end{aligned} \tag{14}$$

The state response norm is given as follows:

$$\begin{aligned}||\mathbf{x}(l)|| \le \lambda_{\max} &\left\{\mathbf{A}^{\tau_{\max}} + \sum_{r=0}^{\tau_{\max}-1} \mathbf{A}^r\mathbf{BK}\right\} \times \left|\left| (\mathbf{A} + \mathbf{BK})^{\tau_k} \right.\right. \\ &\times \left(\mathbf{A}^{\tau_{k-1}} + \sum_{r=0}^{\tau_{k-1}-1} \mathbf{A}^r\mathbf{BK}\right) \cdots \left(\mathbf{A} + \mathbf{BK}^{\tau_1}\right) \left.\right|| \, \|\mathbf{x}_0\|.\end{aligned} \tag{15}$$

If the eigenvalues of both $(\mathbf{A} + \mathbf{BK})^{\tau_i}$ and $(\mathbf{A}^{\tau_i} + \sum_{r=0}^{\tau_i-1} \mathbf{A}^r\mathbf{BK})$ are inside the unity circle for all $\tau_i \in [\tau_{\min}, \tau_{\max}], i \in \{0, 1, \ldots, k+1\}$, the convergence of the matrix products is guaranteed. In view of the fact that the original closed-loop system $\mathbf{A} + \mathbf{BK}$ is stable, all the eigenvalues of the matrix $(\mathbf{A} + \mathbf{BK})^{\tau_i}$ are inside the unity circle. Therefore, the system (10) is globally asymptotically stable if the eigenvalues of the matrices $(\mathbf{A}^{\tau_i} + \sum_{r=0}^{\tau_i-1} \mathbf{A}^r\mathbf{BK})$ are inside the unity circle for all $\tau_i \in [\tau_{\min}, \tau_{\max}], i \in \{0, 1, \ldots, k+1\}$.

Thus, sufficient conditions for the globally asymptotical stability of the system (10) are obtained. ■

With this theorem, we are able to find the largest interval $[\tau_{\min}, \tau_{\max}]$ for τ_i, below which the globally asymptotical stability of the system (10) can be guaranteed. By calculating the maximum eigenvalues for $(\mathbf{A}^{\tau_i} + \sum_{r=0}^{\tau_i-1} \mathbf{A}^r\mathbf{BK})$ with τ_i, the $\tau_{\max}$ will be the values of τ_i that $(\mathbf{A}^{\tau_i} + \sum_{r=0}^{\tau_i-1} \mathbf{A}^r\mathbf{BK})$ have the maximum eigenvalues outside of unity circle for the first time.

B. Mean-Square Stability for the Random Sojourn Times With Independent Identical Distributions

In this section, we study the stochastic stability (mean-square stability) of the power system (10) with random sojourn times $\{\tau_1, \tau_2, \ldots, \tau_i, \ldots, \tau_{k+1}\}$ which follow the identical probability density function (p.d.f) $p(\tau_i)$ for all $i \in \{1, 2, \ldots, k+1\}$.

Definition 2: For IID sojourn times which follow the p.d.f $p(\tau_i)$, for all $i \in \{1, 2, \ldots, k+1\}$, the state trajectory $\mathbf{x}(l)$ in system (10) with initial conditions $\mathbf{x}(t_0) = \mathbf{x}_0$ and $\theta_{t_0} = \theta_0 \in \Theta = \{0, 1\}$ is mean square stable if $\mathbf{x}(l)$ satisfies $\lim_{l\to\infty} E\{||\mathbf{x}(l, t_0, \mathbf{x}_0||^2)\} = 0$.

We give sufficient conditions under which the system (10) is mean-square stable with random sojourn times.

Theorem 2: The system (10), with sojourn times τ_i, $i \in \{1, 2, \ldots, k+1\}$, which follow the identical probability density function (p.d.f) $p(\tau_i)$, is mean-square stable, if the following inequalities hold for all $i \in \{1, 2, \ldots, k+1\}$.

1) The expected maximum singular value of the matrix $\Psi(\tau_i)$ is convergent, that is $\sum_{\tau_i=1}^{\infty} p(\tau_i)\sigma_{\max}(\Psi(\tau_i)) < \infty$, where $\Psi(\tau_i) = (\mathbf{A}^{\tau_i} + \sum_{r=0}^{\tau_i-1} \mathbf{A}^r\mathbf{BK})$.
2) The expected maximum singular value of the matrix $\Upsilon(\tau_i)$ is convergent, that is $\sum_{\tau_i=1}^{\infty} p(\tau_i)\sigma_{\max}(\Upsilon(\tau_i)) < \infty$, where $\Upsilon(\tau_i) = (\mathbf{A} + \mathbf{BK})^{\tau_i}$.
3) $\sum_{\tau_i=1}^{\infty} p(\tau_i)\sigma_{\max}(\Upsilon(\tau_i))^2 < \infty$.
4) $\sum_{\tau_i=1}^{\infty} p(\tau_i)\sigma_{\max}(\Psi(\tau_i))^2 < \infty$, where, $\sigma_{\max}(*)$ denotes the maximum singular value of the matrix $*$.

Proof: We consider the initial conditions $\mathbf{x}(t_0) = \mathbf{x}_0$ and $\theta_{t_0} \in \Theta = \{0, 1\}$. For each initial state case, the final state can be either $\theta_{t_k} = 0$ or $\theta_{t_k} = 1$. The sojourn time sequence during the time interval $[t_0, t_{k+1})$ is denoted by $\{\tau_1, \tau_2, \ldots, \tau_i, \ldots, \tau_k, \tau_{k+1}\}$. On the last state interval $[t_k, t_{k+1}]$, for any $l \in [t_k, t_{k+1})$, the state $\mathbf{x}(l)$ of the system (10) has the following forms.

1) When the initial state of the communication channel is OFF and the finial state is OFF, the $\mathbf{x}(l)$ has the following form:

$$\mathbf{x}(l) = \left(\mathbf{A}^{l-t_k} + \sum_{r=0}^{l-t_k-1} \mathbf{A}^r\mathbf{BK}\right) \times (\mathbf{A}+\mathbf{BK})^{\tau_k} \cdots \times (\mathbf{A}+\mathbf{BK})^{\tau_2} \times \left(\mathbf{A}^{\tau_1} + \sum_{r=0}^{\tau_1-1} \mathbf{A}^r\mathbf{BK}\right)\mathbf{x}_0. \quad (16)$$

Let $\Phi(\tau_k) = (\mathbf{A}+\mathbf{BK})^{\tau_k}\cdots(\mathbf{A}+\mathbf{BK})^{\tau_2}(\mathbf{A}^{\tau_1} + \sum_{r=0}^{\tau_1-1}\mathbf{A}^r\mathbf{BK})$, $\Xi(l) = \mathbf{A}^{l-t_k} + \sum_{r=0}^{l-t_k-1}\mathbf{A}^r\mathbf{BK}$. The expectation of the square norm of $\mathbf{x}(l)$ is

$$E\left\{||\mathbf{x}(l)||^2\right\} = E\left\{\mathbf{x}_0^T\left[\Phi(\tau_k)^T\,\Xi(l)^T\Xi(l)\Phi(\tau_k)\right]\mathbf{x}_0\right\} \le E\left\{\sigma_{\max}\left(\mathbf{A}^{\tau_{k+1}} + \sum_{r=0}^{\tau_{k+1}-1}\mathbf{A}^r\mathbf{BK}\right)\right\} E\left\{\Phi(\tau_k)^T\Phi(\tau_k)\right\}||\mathbf{x}_0||^2 \quad (17)$$

where, $\sigma_{\max}(*)$ denotes the maximum singular value of the matrix $*$.

Due to

$$E\left\{\Phi(\tau_k)^T\Phi(\tau_k)\right\} \le E\left\{\left\|(\mathbf{A}+\mathbf{BK})^{\tau_k}\right\|^2\right\} \times \cdots \times E\left\{\left|\left|\mathbf{A}^{\tau_1} + \sum_{r=0}^{\tau_1-1}\mathbf{A}^r\mathbf{BK}\right|\right|^2\right\} \quad (18)$$

we have the following inequality:

$$E\left\{||\mathbf{x}(l)||^2\right\} \le E\left\{\sigma_{\max}\left(\mathbf{A}^{\tau_{k+1}} + \sum_{r=0}^{\tau_{k+1}-1}\mathbf{A}^r\mathbf{BK}\right)\right\} \times \cdots \times E\left\{\left|\left|\mathbf{A}^{\tau_1} + \sum_{r=0}^{\tau_1-1}\mathbf{A}^r\mathbf{BK}\right|\right|^2\right\}||\mathbf{x}_0||^2. \quad (19)$$

Since all the sojourn times $\tau_i, i \in \{0, 1, \ldots, k+1\}$ follow the identical p.d.f $p(\tau_i)$, if the following inequalities hold true:

$$E\left\{\sigma_{\max}\left(\Psi(\tau_i)\right)\right\} = \sum_{\tau_i=1}^{\infty} p(\tau_i)\,\sigma_{\max}\left(\Psi(\tau_i)\right) < \infty \quad (20)$$

where, $\Psi(\tau_i) = (\mathbf{A}^{\tau_i} + \sum_{r=0}^{\tau_i-1}\mathbf{BK})$, $p(\tau_i)$ is the probability density function of τ_i, and

$$E\left\{\left|\left|(\mathbf{A}+\mathbf{BK})^{\tau_i}\right|\right|^2\right\} = \sum_{\tau_i=1}^{\infty} p(\tau_i)\,||\Upsilon(\tau_i)||^2 < \infty \quad (21)$$

where, $\Upsilon(\tau_i) = (\mathbf{A}+\mathbf{BK})^{\tau_i}$, and

$$E\left\{\left|\left|\mathbf{A}^{\tau_i} + \sum_{r=0}^{\tau_i-1}\mathbf{BK}\right|\right|^2\right\} = \sum_{\tau_i=1}^{\infty} p(\tau_i)\,||\Psi(\tau_i)||^2 < \infty \quad (22)$$

then, $E\left\{||\mathbf{x}(l)||^2\right\} < \infty$ and $\sum_{l=0}^{\infty} E\left\{||\mathbf{x}(l)||^2\right\} < \infty$. Therefore, system (10) is mean-square stable.

2) When the initial state of the communication channel is OFF and the finial state is ON, the $\mathbf{x}(l)$ has the following form:

$$\mathbf{x}(l) = (\mathbf{A}+\mathbf{BK})^{l-t_k} \times \left(\mathbf{A}^{\tau_k} + \sum_{r=0}^{\tau_k-1}\mathbf{BK}\right) \times \cdots \times \left(\mathbf{A}^{\tau_1} + \sum_{r=0}^{\tau_1-1}\mathbf{A}^r\mathbf{BK}\right)\mathbf{x}_0. \quad (23)$$

Let $\Phi(\tau_k) = (\mathbf{A}^{\tau_k} + \sum_{r=0}^{\tau_k-1}\mathbf{BK})\cdots(\mathbf{A}+\mathbf{BK})^{\tau_2}(\mathbf{A}^{\tau_1} + \sum_{r=0}^{\tau_1-1}\mathbf{A}^r\mathbf{BK})$. The expectation of the square norm of $\mathbf{x}(l)$ is

$$E\left\{||\mathbf{x}(l)||^2\right\} = E\left\{\mathbf{x}_0^T\left[\Phi(\tau_k)^T\left((\mathbf{A}+\mathbf{BK})^{l-t_k}\right)^T (\mathbf{A}+\mathbf{BK})^{l-t_k}\Phi(\tau_k)\right]\mathbf{x}_0\right\} \le E\{\sigma_{\max}(\mathbf{A}+\mathbf{BK})^{\tau_{k+1}}\} E\left\{\Phi(\tau_k)^T\Phi(\tau_k)\right\}||\mathbf{x}_0||^2 \quad (24)$$

where $\sigma_{\max}(*)$ denotes the maximum singular value of the matrix $*$.

Due to

$$E\left\{\Phi(\tau_k)^T\Phi(\tau_k)\right\} \le E\left\{\left|\left|\mathbf{A}^{\tau_k} + \sum_{r=0}^{\tau_k-1}\mathbf{BK}\right|\right|^2\right\} \times \cdots \times E\left\{\left|\left|\mathbf{A}^{\tau_1} + \sum_{r=0}^{\tau_1-1}\mathbf{A}^r\mathbf{BK}\right|\right|^2\right\} \quad (25)$$

if the inequalities (21) and (22) in case 1) hold true and the following inequality holds:

$$E\left\{\sigma_{\max}\left(\Upsilon(\tau_i)\right)\right\} = \sum_{\tau_i=1}^{\infty} p(\tau_i)\,\sigma_{\max}\left(\Upsilon(\tau_i)\right) < \infty \quad (26)$$

where, $\Upsilon(\tau_i) = (\mathbf{A}+\mathbf{BK})^{\tau_i}$, and $p(\tau_i)$ is the probability density function of τ_i, then $E\left\{||\mathbf{x}(l)||^2\right\} < \infty$ and $\sum_{l=0}^{\infty} E\left\{||\mathbf{x}(l)||^2\right\} < \infty$. Therefore, system (10) is mean-square stable.

3) When the initial state of the communication channel is ON and the finial state is OFF, the $\mathbf{x}(l)$ has the following form:

$$\mathbf{x}(l) = \left(\mathbf{A}^{l-t_k} + \sum_{r=0}^{l-t_k-1}\mathbf{A}^r\mathbf{BK}\right) \times (\mathbf{A}+\mathbf{BK})^{\tau_k} \cdots \times \left(\mathbf{A}^{\tau_2} + \sum_{r=0}^{\tau_2-1}\mathbf{A}^r\mathbf{BK}\right)(\mathbf{A}+\mathbf{BK})^{\tau_1}\mathbf{x}_0. \quad (27)$$

Let $\Phi(\tau_k) = (\mathbf{A}+\mathbf{BK})^{\tau_k}\cdots(\mathbf{A}^{\tau_2} + \sum_{r=0}^{\tau_2-1}\mathbf{A}^r\mathbf{BK})(\mathbf{A}+\mathbf{BK})^{\tau_1}$, and $\Xi(l) = \mathbf{A}^{l-t_k} + \sum_{r=0}^{l-t_k-1}\mathbf{A}^r\mathbf{BK}$. The expectation of the square norm of $\mathbf{x}(l)$ is

$$E\left\{||\mathbf{x}(l)||^2\right\} = E\left\{\mathbf{x}_0^T\left[\Phi(\tau_k)^T\,\Xi(l)^T\Xi(l)\Phi(\tau_k)\right]\mathbf{x}_0\right\}$$

$$\leq E\left\{\sigma_{\max}\left(\mathbf{A}^{\tau_{k+1}}+\sum_{r=0}^{\tau_{k+1}-1}\mathbf{A}^{r}\mathbf{BK}\right)\right\} E\left\{\Phi(\tau_k)^T\Phi(\tau_k)\right\}||\mathbf{x}_0||^2 \quad (28)$$

where, $\sigma_{\max}(*)$ denotes the maximum singular value of the matrix $*$.

If the inequalities (20), (21), and (22) in case (i) hold, then $E\left\{||\mathbf{x}(l)||^2\right\} < \infty$ and $\sum_{l=0}^{\infty} E\left\{||\mathbf{x}(l)||^2\right\} < \infty$. Therefore, system (10) is mean-quare stable.

4) When the initial state of the communication channel is ON and the finial state is ON, then

$$\mathbf{x}(l) = (\mathbf{A}+\mathbf{BK})^{l-t_k} \times \left(\mathbf{A}^{\tau_{k-1}}+\sum_{r=0}^{\tau_{k-1}}\mathbf{A}^{r}\mathbf{BK}\right)\cdots \times\left(\mathbf{A}^{\tau_2}+\sum_{r=0}^{\tau_2-1}\mathbf{A}^{r}\mathbf{BK}\right)\times(\mathbf{A}+\mathbf{BK})^{\tau_1}\mathbf{x}_0. \quad (29)$$

Let $\Phi(\tau_k) = (\mathbf{A}^{\tau_k}+\sum_{r=0}^{\tau_k-1}\mathbf{BK})\cdots(\mathbf{A}^{\tau_2}+\sum_{r=0}^{\tau_2-1}\mathbf{A}^{r}\mathbf{BK}(\mathbf{A}+\mathbf{BK})^{\tau_1}$, and $\Xi(l) = (\mathbf{A}+\mathbf{BK})^{l-t_k}$. The expectation of the square norm of $\mathbf{x}(l)$ is

$$E\left\{||\mathbf{x}(l)||^2\right\} = E\left\{\mathbf{x}_0^T\left[\Phi(\tau_k)^T\Xi(l)^T\Xi(l)\Phi(\tau_k)\right]\mathbf{x}_0\right\} \leq E\{\sigma_{\max}\left((\mathbf{A}+\mathbf{BK})^{\tau_{k+1}}\right)\} E\left\{\Phi(\tau_k)^T\Phi(\tau_k)\right\}||\mathbf{x}_0||^2 \quad (30)$$

where, $\sigma_{\max}(*)$ denotes the maximum singular value of the matrix $*$.

If the inequalities (20), (21), and (22) in case (i) hold, then $E\left\{||\mathbf{x}(l)||^2\right\} < \infty$ and $\sum_{l=0}^{\infty} E\left\{||\mathbf{x}(l)||^2\right\} < \infty$. Therefore, system (10) is mean-square stable.

If $\Psi(\tau_i)$ and $\Upsilon(\tau_i)$ are matrices with their ranks m and n, respectively, their singular values are denoted by $\sigma_j(\Psi(\tau_i))$ and $\sigma_j(\Upsilon(\tau_i))$. According to the properties of the singular values [36], $||\Psi(\tau_i)||^2 = \sum_{j=1}^{m}\sigma_j^2(\Psi(\tau_i))$, and $||\Upsilon(\tau_i)||^2 = \sum_{j=1}^{n}\sigma_j^2(\Upsilon(\tau_i))$. Thus, the condition (21) is equivalent to

$$E\left\{\left|\left|(\mathbf{A}+\mathbf{BK})^{\tau_i}\right|\right|^2\right\} = \sum_{\tau_i=1}^{\infty}p(\tau_i)||\Upsilon(\tau_i)||^2 = \sum_{\tau_i=1}^{\infty}p(\tau_i)\sum_{j=1}^{m}\sigma_j^2(\Upsilon(\tau_i)) \leq m\sum_{\tau_i=1}^{\infty}p(\tau_i)\sigma_{\max}(\Upsilon(\tau_i))^2 < \infty \quad (31)$$

and the condition (22) is equivalent to

$$E\left\{\left|\left|\mathbf{A}^{\tau_i}+\sum_{r=0}^{\tau_i-1}\mathbf{BK}\right|\right|^2\right\} = \sum_{\tau_i=1}^{\infty}p(\tau_i)||\Psi(\tau_i)||^2 = \sum_{\tau_i=1}^{\infty}p(\tau_i)\sum_{j=1}^{n}\sigma_j^2(\Psi(\tau_i)) \leq n\sum_{\tau_i=1}^{\infty}p(\tau_i)\sigma_{\max}(\Psi(\tau_i))^2 < \infty. \quad (32)$$

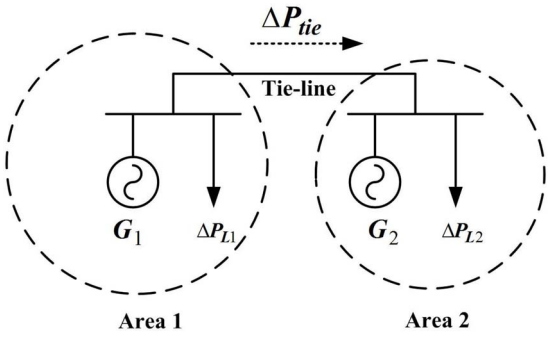

Fig. 5. Two-area power system.

In summary, if the inequalities (20), (26), (31), and (32) hold, the system (10) is mean-square stable. This completes the proof. ■

A maximum singular value is usually used as an important indicator of the robust stability of linear systems with uncertainties [37], [38]. Therefore, the expected maximum singular values of the matrices can be used as the upper bounds for the stochastic stability of the system (10).

IV. Performance Analysis of Two-Area Power System

In this section, a two-area power system model is used to evaluate the effects of CR networks on the system performance. For stochastic sojourn time cases, both uniform and geometric p.d.f sojourn time processes are simulated to evaluate their influences to the dynamic performance of the power system. The two processes are firstly evaluated under two different initial frequency changes resulted from load changes. Then, they are investigated under two different tie-line power situations. For the arbitrary sojourn time case, the largest sojourn time interval below which the asymptotical stability can be guaranteed is calculated. For the stochastic sojourn time case, the expected maximum singular values are calculated for the sojourn times of CR networks follow the uniform probability distribution. All the numerical simulations are run in MATLAB R2012a in a computer with 2.66 GHz CPU and 8.00 GB RAM. In this paper, 100 MVA is chosen as the base unit for per unit (pu) calculations. The two-area power system is shown in Fig. 5 and its parameters are shown in Table IV and in the Appendix. Its state-space model is given as follows:

$$\dot{\mathbf{x}} = \mathbf{A_c}\mathbf{x} + \mathbf{B_c}\mathbf{u} \quad (33)$$

where

$$\mathbf{x} = \begin{bmatrix}\Delta P_{\text{tie}} & \Delta f_1 & \Delta P_{m_1} & \Delta P_{v_1} & \Delta f_2 & \Delta P_{m_2} & \Delta P_{v_2}\end{bmatrix}^T$$

$$\mathbf{u} = \begin{bmatrix}\Delta P_{c_1} & \Delta P_{c_2}\end{bmatrix}^T$$

$$\mathbf{A_c} = \begin{bmatrix} 0 & 0.545 & 0 & 0 & -0.545 & 0 & 0 \\ -5 & -0.07 & 5 & 0 & 0 & 0 & 0 \\ 0 & 0 & -2.5 & 2.5 & 0 & 0 & 0 \\ 0 & -5.21 & 0 & -12.5 & 0 & 0 & 0 \\ 6 & 0 & 0 & 0 & -0.05 & 6 & 0 \\ 0 & 0 & 0 & 0 & 0 & -2.78 & 2.78 \\ 0 & 0 & 0 & 0 & -6.94 & 0 & -16.67 \end{bmatrix}$$

$$\mathbf{B_c} = \begin{bmatrix} 0 & 0 & 0 & 12.5 & 0 & 0 & 0 \\ 0 & 0 & 0 & 0 & 0 & 0 & 16.67 \end{bmatrix}^T.$$

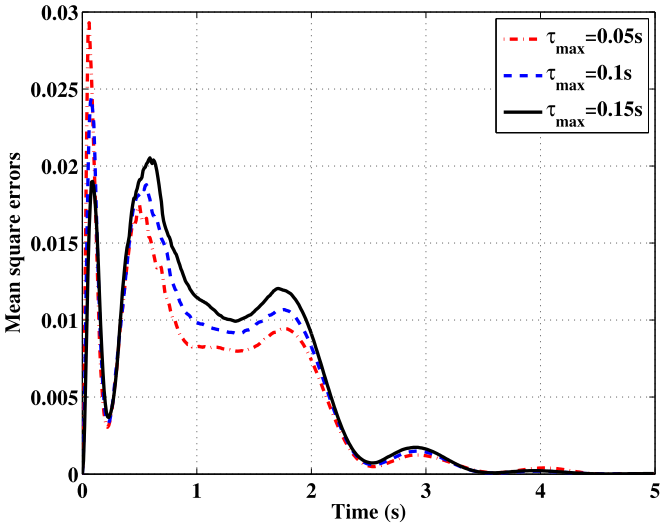

Fig. 6. Mean-square errors of the power system states with uniform p.d.f sojourn times in Case 1.

With the sampling period $h = 0.01s$, the sampled system is denoted by

$$\mathbf{x}(k+1) = \mathbf{A}\mathbf{x}(k) + \mathbf{B}\mathbf{u}(k) \tag{34}$$

where, $\mathbf{A} = e^{0.01\mathbf{A_c}}$, $\mathbf{B} = \int_0^{0.01} e^{\mathbf{A_c}\tau}\mathbf{B_c}d\tau$. A discrete-time linear quadratic regulator (LQR) is designed for this power system $\mathbf{u} = \mathbf{K}\mathbf{x}$. A CR network is used as the communication channel in the AGC of the power system and its state $\theta_k \in \Theta = \{0, 1\}$, where $\Theta = \{0, 1\}$ is the state space of θ_k, 0 denoting OFF state of the channel, 1 denoting ON state. The closed-loop system $\mathbf{x}(k+1) = (\mathbf{A} + \mathbf{BK})\mathbf{x}(k)$ has the following switched system form during the interval $l \in [t_k, t_{k+1})$ when $\theta_{t_k} \in \{0, 1\}$:

$$\mathbf{x}(l) = \begin{cases} (\mathbf{A}+\mathbf{BK})^{l-t_k}\,\mathbf{x}(t_k), \theta_{t_k} = 1 \\ \left(\mathbf{A}^{l-t_k} + \sum_{r=0}^{l-t_k-1} \mathbf{A}^r\mathbf{BK}\right)\mathbf{x}(t_k), \theta_{t_k} = 0. \end{cases} \tag{35}$$

Firstly, the effects of CR networks with uniform p.d.f sojourn times on the power system performance are evaluated. The following mean-square error (MSE) of the state of the power system is used as the metric of its dynamic performance:

$$\mathrm{MSE}(k) = \frac{1}{N}\sum_{i=1}^{N} (\mathbf{x}(k) - \mathbf{x}_0(k))^T (\mathbf{x}(k) - \mathbf{x_0}(k)) \tag{36}$$

where $\mathbf{x_0}(k)$ is the original power system state at kth time instant without any disturbances, and $\mathbf{x}(k)$ is the system state when a CR network is used, and N denotes how many times the simulations run. Here, the simulations run 500 times and the time horizon of each simulation is 5 s. In order to evaluate different load changes and tie-line power flows in the power system, four different initial conditions are considered.

Case 1: $\Delta f_1(0) = 1.5$ Hz in Area 1 and $\Delta f_2(0) = 0.5$ Hz in Area 2.

Case 2: $\Delta f_1(0) = 2$ Hz in Area 1 and $\Delta f_2(0) = 1$ Hz in Area 2.

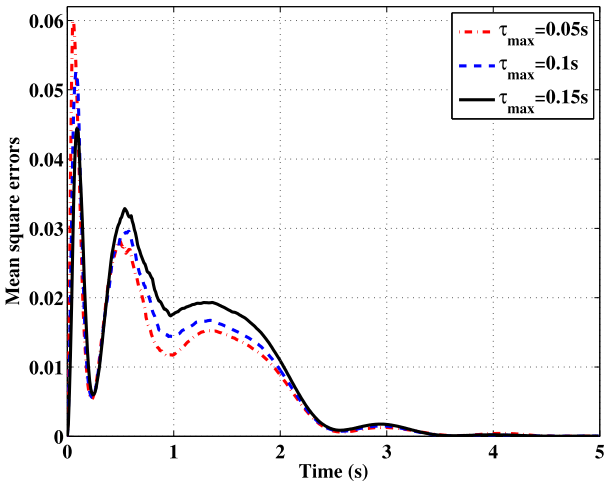

Fig. 7. Mean-square errors of the power system states with uniform p.d.f sojourn times in Case 2.

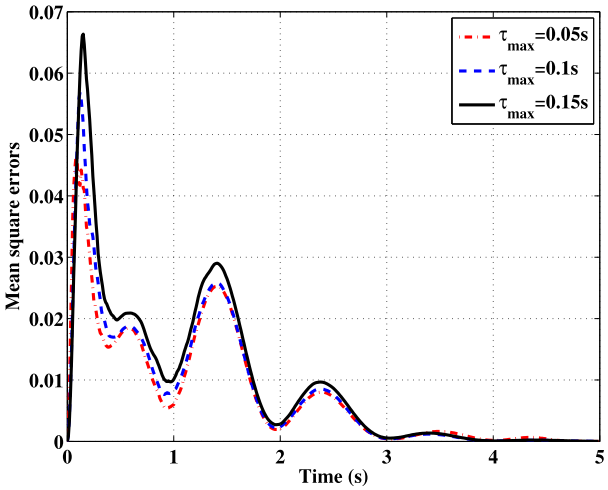

Fig. 8. Mean-square errors of the power system states with uniform p.d.f sojourn times in Case 3.

Case 3: $\Delta P_{\mathrm{tie}}^{12}(0) = 0.5(pu)$.

Case 4: $\Delta P_{\mathrm{tie}}^{12}(0) = 1(pu)$.

The MSEs of the states of the power system with random sojourn times which follow uniform p.d.f for the four cases are shown in Figs. 6–9. By comparing Figs. 6 and 7, it can be seen that the system performance becomes much worse when the load changes in two areas are bigger. Also, for both cases, the system performance is the worst over the CR network with the biggest $\tau_{\max}$. When tie line power are considered, the comparison of Figs. 8 and 9 shows that the system performance is worse when the larger tie-line power are transferring between area 1 and 2. Moreover, for these two tie-line power cases, the system performance is the worst over the CR network with the biggest $\tau_{\max}$. According to these results, with a given maximum mean-square error that a power system can endure, the maximum sojourn time that CR networks should not be exceeded can be estimated when a CR network is designed for a smart grid.

Then, the effects of CR networks with geometric p.d.f sojourn times on the power system performance are evaluated.

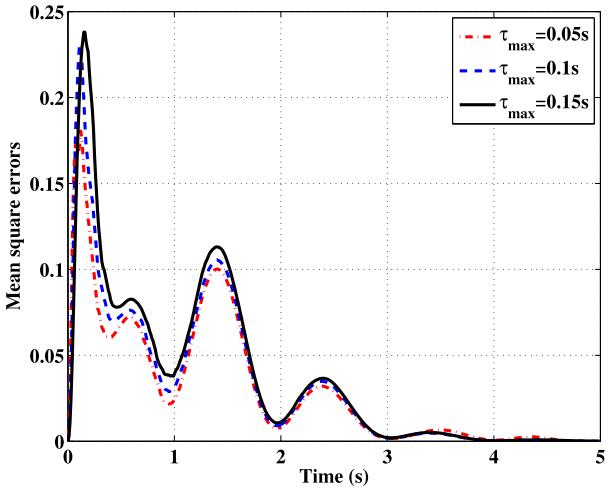

Fig. 9. Mean-square errors of the power system states with uniform p.d.f sojourn times in Case 4.

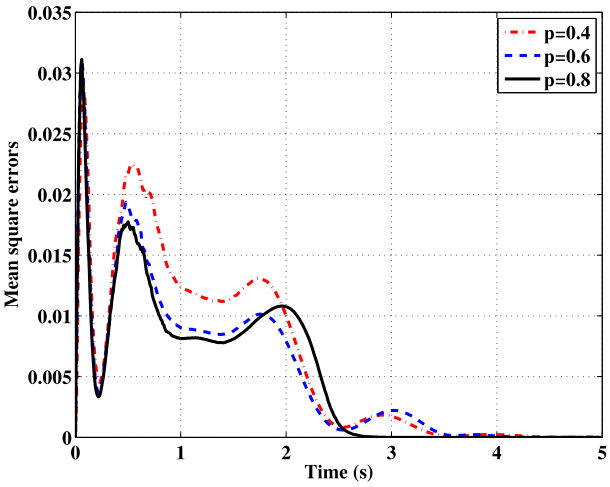

Fig. 10. Mean-square errors of the power system states with geometric p.d.f sojourn times in Case 1.

The MSEs of the states of the power system with random sojourn times which follow geometric p.d.f for the four cases are shown in Figs. 10–13, while the parameter p denotes the success probability of the geometric p.d.f. When load changes are considered, the comparison of Figs. 10 and 11 tells that the system performance becomes worse when the load changes in two areas of the power system are larger. Also, it can be seen from the two figures that the system performance is the worst over the CR network with the smallest success probability of the geometric p.d.f ($p = 0.4$). When tie line power changes are taken into accounts, by comparing Figs. 12 and 13, it is shown that the system performance is worse when the larger tie-line power are transferring between area 1 and 2. Furthermore, for these two tie-line power cases, the system performance is the worst over the CR network with the smallest success probability of the geometric p.d.f ($p = 0.4$). According to these results, with a given maximum mean-square error that a power system can endure, the smallest successful transmission rate that CR networks should be reached can be estimated when a CR network is designed for a smart grid.

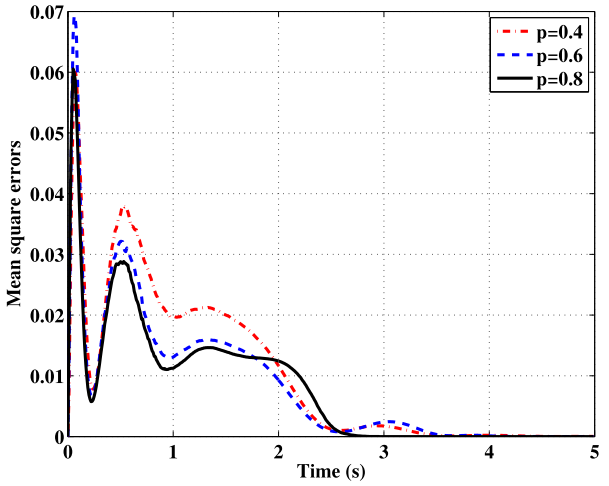

Fig. 11. Mean-square errors of the power system states with geometric p.d.f sojourn times in Case 2.

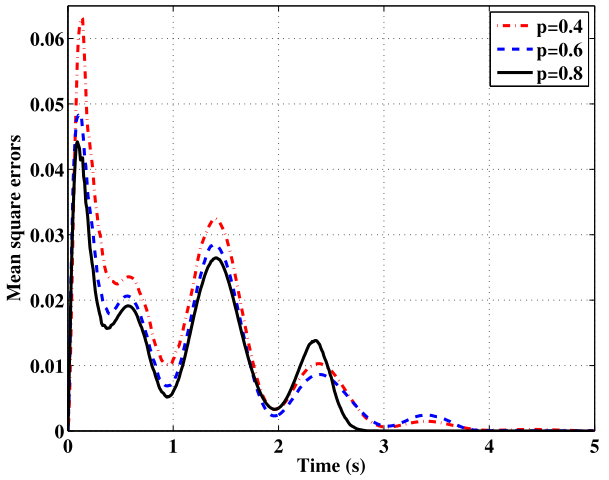

Fig. 12. Mean-square errors of the power system states with geometric p.d.f sojourn times in Case 3.

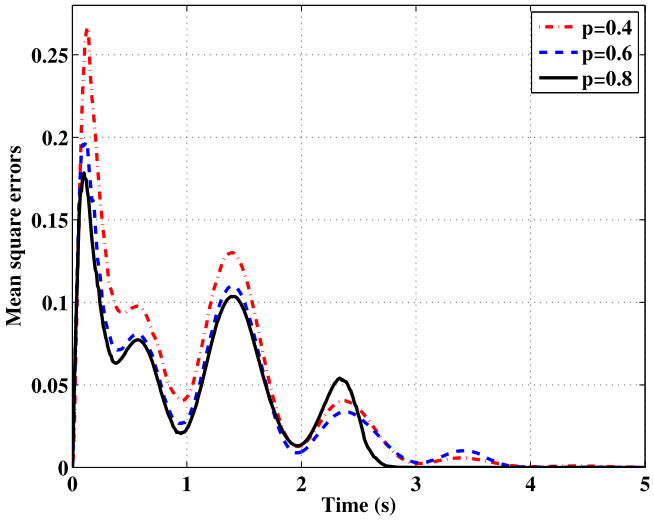

Fig. 13. Mean-square errors of the power system states with geometric p.d.f sojourn times in Case 4.

Furthermore, the maximum sojourn time is calculated for the arbitrary but bounded sojourn time case according to Theorem 1. Maximum eigenvalues with different sampling

TABLE I
MAXIMUM EIGENVALUES OF THE MATRICES $\lambda(\Psi(\tau))$ WITH DIFFERENT SAMPLING PERIODS h

τ (time steps)	$\lambda(\Psi(\tau))$ $(h = 0.05)$	$\lambda(\Psi(\tau))$ $(h = 0.1)$	$\lambda(\Psi(\tau))$ $(h = 0.5)$	$\lambda(\Psi(\tau))$ $(h = 1)$
1	0.9262 + 0.1350i	0.8570 + 0.2583i	-0.0048 + 0.7843i	-0.6495 + 0.0394i
2	0.8348 + 0.2505i	0.6518 + 0.4406i	-0.5991	0.4186 + 0.1048i
3	0.7232 + 0.3090i	0.4349 + 0.4604i	0.1437 + 0.4700i	-0.2621 + 0.0905i
4	-0.8864	**-1.0253**	0.4317 + 0.1415i	0.1678 + 0.0719i
5	**-1.4904**	-1.7214	-0.0948 + 0.4236i	-0.1022 + 0.0846i
6	-2.2304	-2.4082	0.4418	0.0689 + 0.0252i
7	-3.0881	-3.0435	0.4698	-0.0469 + 0.0655i
8	-4.0348	-3.6285	0.5387	0.0472
9	-5.0532	-4.1530	0.6074	-0.0790
10	-6.1287	-4.6057	0.6800	0.0292
11	-7.2484	-4.9816	0.7521	-0.1144
12	-8.4005	-5.2823	0.8226	0.0157
13	-9.5745	-5.5144	0.8880	-0.1470
14	-10.7605	-5.6879	0.9550	0.0073
15	-11.9499	-5.8148	**1.0255**	0.0000
16	-13.1349	-5.9083	1.0955	0.0027

TABLE II
EXPECTED MAXIMUM SINGULAR VALUES $\sigma_{\max}(\Psi(\tau))$ WITH THE MAXIMUM SOJOURN TIMES $\tau_{\max}$ UNDER SAMPLING PERIOD h

τ_{max} time steps	$\sigma_{max}(\Psi(\tau))$ $h = 0.05$	$\sigma_{max}(\Psi(\tau))$ $h = 0.1$	$\sigma_{max}(\Psi(\tau))$ $h = 0.5$	$\sigma_{max}(\Psi(\tau))$ $h = 1$
1	1.7391	2.1950	2.7718	1.2238
2	11.7573	9.6373	2.6534	1.3902
3	15.2699	12.1562	2.7059	1.2699
4	17.2216	13.5203	2.5066	1.2856
5	18.5933	14.4820	2.4528	1.2717
6	19.7057	15.2893	2.4636	1.2775
7	20.6924	16.0455	2.4849	1.2872
8	21.6170	16.7984	2.5049	1.2983
9	22.5131	17.5686	2.5339	1.3148
10	23.4002	18.3613	2.5719	1.3307

TABLE III
EXPECTED MAXIMUM SINGULAR VALUES $\sigma_{\max}(\Upsilon(\tau))$ WITH THE MAXIMUM SOJOURN TIMES $\tau_{\max}$ UNDER SAMPLING PERIOD h

τ_{max} time steps	$\sigma_{max}(\Upsilon(\tau))$ $h = 0.05$	$\sigma_{max}(\Upsilon(\tau))$ $h = 0.1$	$\sigma_{max}(\Upsilon(\tau))$ $h = 0.5$	$\sigma_{max}(\Upsilon(\tau))$ $h = 1$
1	1.7391	2.1950	2.7718	1.2238
2	1.9304	2.3592	2.0105	0.9436
3	2.0618	2.4618	1.8759	0.7941
4	2.1604	2.5110	1.5547	0.6828
5	2.2368	2.5116	1.4447	0.5965
6	2.2953	2.4707	1.2699	0.5270
7	2.3380	2.3975	1.1759	0.4701
8	2.3663	2.3022	1.0582	0.4227
9	2.3814	2.1949	0.9824	0.3828
10	2.3844	2.0856	0.8987	0.3490

periods are listed in Table I. From this table, we can obtain the maximum sojourn times below which the asymptotical stability of the power system is guaranteed with different sampling periods, by checking the first time when maximum eigenvalues are outside unity circle which are indicated as bolded and colored numbers in the table.

Finally, we consider a stochastic sojourn time case. The stochastic sojourn times are assumed to follow the uniform p.d.f within $[\tau_{\min}, \tau_{\max}]$. This kind of sojourn times has been used to model the sojourn time in CRs [13]. The relationships between the expected maximum singular values and the maximum sojourn time intervals with different sampling periods have been shown in Tables II and III. These tables are able to give suggestions that how to design the CR network to guarantee the stochastic stability of the AGC of the smart grid, according to the corresponding relationships between the maximum sojourn time intervals and the expected maximum singular values.

V. CONCLUSION

In this paper, we have studied the modeling and stability analysis issues of the AGC of smart grids for which CR networks are used as the communication and networking infrastructure. By modeling the CR network as an On–Off switch with sojourn times, a new switched power system model has been proposed for the AGC of a smart grid. The stability of the AGC of the smart grid has been studied for two main types of CR networks: 1) the sojourn time is arbitrary but bounded and 2) the sojourn time follows an IID process. For the first type of CR networks, sufficient conditions have been derived for ensuring the asymptotical stability of the AGC of the smart grid. For the second one, sufficient conditions have been found to guarantee the mean-square stability of the AGC of the smart grid. Simulation results show how the conflict between PU and SU traffic affects the dynamic performance of the smart grid. They also indicate that the degraded dynamic performance and the developed sufficient conditions can be used to estimate the

TABLE IV
TWO-AREA POWER SYSTEM PARAMETERS

Area 1	Area 2
$T_{ch_1} = 0.4s$	$T_{ch_2} = 0.36s$
$T_{g_1} = 0.08s$	$T_{g_2} = 0.30s$
$R_1 = 2.4Hz/pu$	$R_2 = 2.4Hz/pu$
$D_1 = 0.014pu/Hz$	$D_2 = 0.0084pu/Hz$
$2H_1 = 0.2pu \cdot s$	$2H_2 = 0.1667pu \cdot s$
$T_{12} = 0.08678$	$T_{21} = 0.08678$

maximum sojourn time in the design of CR networks in order to ensure the stability of the AGC of the smart grid.

In this paper, it has been found CR networks could jeopardize the dynamic performance of the AGC of smart grids. Therefore, the future work will be devoted to how to improve the AGC performance when CR networks are used in smart grids. To achieve this purpose, the following two directions should be considered.

1) Design control methods to improve the robustness of the AGC to the interruptions caused by CR networks. For example, since the proposed AGC model is a switched system, control algorithms for randomly switched systems could be adjusted for the CR network situations.
2) Design optimal CR networking protocols to improve the Quality of Service (QoS) of CR networks, including the maximum time delay and the success rate of delivered packets in CR networks.

APPENDIX

The two-area power system parameters are shown in Table IV [33].

REFERENCES

[1] H. Farhangi, "The path of the smart grid," *IEEE Power Energy Mag.*, vol. 8, no. 1, pp. 18–28, Jan./Feb. 2010.

[2] S. M. Amin and B. F. Wollenberg, "Toward a smart grid: Power delivery for the 21st century," *IEEE Power Energy Mag.*, vol. 3, no. 5, pp. 34–41, Sep./Oct. 2005.

[3] F. Bouhafs, M. Mackay, and M. Merabti, "Links to the future: Communication requirements and challenges in the smart grid," *IEEE Power Energy Mag.*, vol. 10, no. 1, pp. 24–32, Jan./Feb. 2012.

[4] D. Karlsson, M. Hemmingsson, and S. Lindahl, "Wide area system monitoring and control—Terminology, phenomena, and solution implementation strategies," *IEEE Power Energy Mag.*, vol. 2, no. 5, pp. 68–76, Sep./Oct. 2004.

[5] E. Santacana, G. Rackliffe, L. Tang, and X. Feng, "Getting smart," *IEEE Power Energy Mag.*, vol. 8, no. 2, pp. 41–48, Mar./Apr. 2010.

[6] V. Gungor *et al.*, "Smart grid technologies: Communication technologies and standards," *IEEE Trans. Ind. Inf.*, vol. 7, no. 4, pp. 529–539, Nov. 2011.

[7] V. Gungor and F. Lambert, "A survey on communication networks for electric system automation," *Comput. Netw.*, vol. 50, no. 7, pp. 877–897, 2006.

[8] V. Gungor and D. Sahin, "Cognitive radio networks for smart grid applications: A promising technology to overcome spectrum inefficiency," *IEEE Veh. Technol. Mag.*, vol. 7, no. 2, pp. 41–46, Jun. 2012.

[9] R. Yu *et al.*, "Cognitive radio based hierarchical communications infrastructure for smart grid," *IEEE Netw.*, vol. 25, no. 5, pp. 6–14, Sep./Oct. 2011.

[10] R. Qiu *et al.*, "Cognitive radio network for the smart grid: Experimental system architecture, control algorithms, security, and microgrid testbed," *IEEE Trans. Smart Grid*, vol. 2, no. 4, pp. 724–740, Dec. 2011.

[11] S. Geirhofer, T. Lang, and B. Sadler, "Cognitive radios for dynamic spectrum access—Dynamic spectrum access in the time domain: Modeling and exploiting white space," *IEEE Commun. Mag.*, vol. 45, no. 5, pp. 66–72, May 2007.

[12] H. Su and X. Zhang, "Cross-layer based opportunistic MAC protocols for QoS provisionings over cognitive radio wireless networks," *IEEE J. Sel. Areas Commun.*, vol. 26, no. 1, pp. 118–129, Jan. 2008.

[13] B. Wang and K. J. R. Liu, "Advances in cognitive radio networks: A survey," *IEEE J. Sel. Topics Signal Process.*, vol. 5, no. 1, pp. 5–23, Feb. 2011.

[14] B. Wang and K. J. R. Liu, "Spectrum sharing in cognitive radio networks with imperfect sensing: A discrete-time Markov model," *Comput. Netw.*, vol. 54, no. 14, pp. 2519–2536, Oct. 2010.

[15] M. Shahraeini, M. Javidi, and M. S. Ghazizadeh, "Comparison between communication infrastructures of centralized and decentralized wide area measurement systems," *IEEE Trans. Smart Grid*, vol. 2, no. 1, pp. 206–211, Mar. 2011.

[16] S. Zhang and V. Vittal, "Design of wide-area power system damping controllers resilient to communication failures," *IEEE Trans. Power Syst.*, vol. 28, no. 4, pp. 4292–4300, Nov. 2013.

[17] J. Liu, A. Gusrialdi, S. Hirche, and A. Monti, "Joint controller-communication topology design for distributed wide area damping control of power system," in *Proc. 18th IFAC World Congr.*, Milan, Italy, Aug. 2011, pp. 519–525.

[18] H. Xin, Z. Qu, J. Seuss, and A. Maknouninejad, "A self organizing strategy for power flow control of photovoltaic generators in a distribution network," *IEEE Trans. Power Syst.*, vol. 36, no. 3, pp. 1462–1473, Aug. 2011.

[19] A. Dominguez-Garcia, C. Hadjicostis, and N. Vaidya, "Resilient networked control of distributed energy resources," *IEEE J. Sel. Areas Commun.*, vol. 30, no. 6, pp. 1137–1148, Jul. 2012.

[20] S. Liu, X. P. Liu, and A. E. Saddik, "Modeling and distributed gain scheduling strategy for load frequency control in smart grids with communication topology changes," *ISA Trans.*, vol. 52, no. 2, pp. 454–461, 2014.

[21] X. Ma, S. Djouadi, and H. Li, "State estimation over a semi-Markov model based cognitive radio system," *IEEE Trans. Wireless Commun.*, vol. 11, no. 7, pp. 2391–2401, Jul. 2012.

[22] X. Ma, H. Li, and S. Djouadi, "Networked system state estimation in smart grid over cognitive radio infrastructures," in *Proc. 2011 45th Annu. Conf. Inf. Sci. Syst. (CISS)*, Baltimore, MD, USA, pp. 1–5.

[23] W. Zhang, M. S. Branicky, and S. M. Phillips, "Stability of networked control systems," *IEEE Control Syst.*, vol. 21, no. 1, pp. 84–99, Feb. 2001.

[24] L. A. Montestruque and P. Antsaklis, "Stability of model-based networked control systems with time-varying transmission times," *IEEE Trans. Autom. Control*, vol. 49, no. 9, pp. 1562–1572, Sep. 2004.

[25] M. Yu, L. Wang, T. Chu, and F. Hao, "An LMI approach to networked control systems with data packet dropout and transmission delays," in *Proc. IEEE Conf. Decis. Control (CDC)*, vol. 4. Atlantis, Bahamas, 2004, pp. 3545–3550.

[26] X. Ye, S. Liu, and P. X. Liu, "Modelling and stabilisation of networked control system with packet loss and time-varying delays," *IET Control Theory Appl.*, vol. 4, no. 6, pp. 1094–1100, 2010.

[27] M. Ilic, L. Xie, U. Khan, and J. Moura, "Modeling of future cyber-physical energy systems for distributed sensing and control," *IEEE Trans. Syst., Man, Cybern. A, Syst., Humans*, vol. 40, no. 4, pp. 825–838, Jul. 2010.

[28] C.-K. Tham and T. Luo, "Sensing-driven energy purchasing in smart grid cyber-physical system," *IEEE Trans. Syst., Man, Cybern., Syst.*, vol. 43, no. 4, pp. 773–784, Jul. 2013.

[29] E. Zio and G. Sansavini, "Vulnerability of smart grids with variable generation and consumption: A system of systems perspective," *IEEE Trans. Syst., Man, Cybern., Syst.*, vol. 43, no. 3, pp. 477–487, May 2013.

[30] M. Huang and S. Dey, "Stability of Kalman filtering with Markovian packet losses," *Automatica*, vol. 43, no. 4, pp. 598–607, 2007.

[31] J. Machovski, J. W. Blalek, and J. R. Bumby, *Power System Dynamics and Stability*. Chichester, U.K.: Wiley, 1998.

[32] A. Venkat, I. Hiskens, J. Rawlings, and S. Wright, "Distributed MPC strategies with application to power system automatic generation control," *IEEE Trans. Control Syst. Technol.*, vol. 16, no. 6, pp. 1192–1206, Nov. 2008.

[33] H. Bevrani, *Robust Power System Frequency Control* (Power Electronics and Power Systems), M. Pai and A. Stankovic, Eds. New York, NY, USA: Springer, 2009.

[34] W.-C. Chan and Y.-Y. Hsu, "Automatic generation control of interconnected power systems using variable-structure controllers," *IEE Proc. C, Gener. Transm. Distrib.*, vol. 128, no. 5, pp. 269–279, Sep. 1981.
[35] A. Oppenheim, A. Willsky, and S. Nawab, *Signals and Systems*. Englewood Cliffs, NJ, USA: Prentice-Hall, 1997.
[36] G. A. F. Seber, *A Matrix Handbook for Statisticians*. Hoboken, NJ, USA: Wiley, 2007.
[37] R. K. Yedavalli, "Improved measures of stability robustness for linear state space models," *IEEE Trans. Autom. Control*, vol. 30, no. 6, pp. 577–579, Jun. 1985.
[38] A. Dickman, "On the robustness of multivariable linear feedback systems in state-space representation," *IEEE Trans. Autom. Control*, vol. 32, no. 5, pp. 407–410, May 1987.

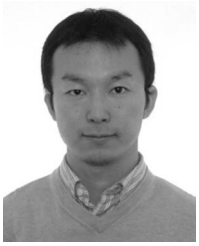

Shichao Liu received the B.Sc. and M.Sc. degrees from Harbin Engineering University, Harbin, China, in 2007 and 2010, respectively, and the Ph.D. degree in electrical and computer engineering from Carleton University, Ottawa, ON, Canada, in September 2014.

His current research interests include networked control system, load frequency control in smart grids, stochastic game theories, energy management, and optimization of microgrids.

Peter X. Liu (M'02–SM'07) received the B.Sc. and M.Sc. degrees from Northern Jiaotong University, Beijing, China, in 1992 and 1995, respectively, and the Ph.D. degree in electrical and computer engineering from the University of Alberta, Edmonton, AB, Canada, in 2002.

He is currently a Canadian Research Chair Professor with the Department of Systems and Computer Engineering, Carleton University, Ottawa, ON, Canada. His current research interests include interactive networked systems and teleoperation, haptics, micromanipulation, robotics, intelligent systems, context-aware intelligent networks, and their applications to biomedical engineering.

Dr. Liu was the recipient of the 2007 Carleton Research Achievement Award, the 2006 Province of Ontario Early Researcher Award, the 2006 Carty Research Fellowship, the Best Conference Paper Award of the 2006 IEEE International Conference on Mechatronics and Automation, and the 2003 Province of Ontario Distinguished Researcher Award. He serves as an Associate Editor for several journals, including the IEEE/ASME TRANSACTIONS ON MECHATRONICS, the IEEE TRANSACTIONS ON AUTOMATION SCIENCE AND ENGINEERING, *Intelligent Service Robotics*, the *International Journal of Robotics and Automation*, *Control and Intelligent Systems*, and the *International Journal of Advanced Media and Communication*. He has served in the organization committees of numerous conferences, including the General Chair of the 2008 IEEE International Workshop on Haptic Audio Visual Environments and their Applications and the General Chair of the 2005 IEEE International Conference on Mechatronics and Automation. He is a member of the Professional Engineers of Ontario.

Abdulmotaleb El Saddik (M'02–SM'13–F'09) received the Ph.D. degree in electrical and computer engineering from the Technical University of Darmstadt, Darmstadt, Germany, in 2001.

He is currently with the School of Information Technology and Engineering, University of Ottawa, Ottawa, ON, Canada, where he is a University Research Chair, a Professor and a Director of the Multimedia Communications Research Laboratory. His current research interests include haptics, service-oriented architectures, collaborative environments, and ambient interactive media and communications.

Dr. El Saddik was the recipient of the National Capital Institute of Telecommunications New Professorship Incentive Award in 2004, the Premier's Research Excellence Award in 2004, the Friedrich Wilhelm-Bessel Research Award from Germany's Alexander von Humboldt Foundation in 2007, and the Professional of the Year Award in 2008. His research has been selected for the Best Paper Award thrice. He serves as an Associate Editor for several journals, including the IEEE TRANSACTIONS ON MULTIMEDIA and the IEEE TRANSACTIONS ON COMPUTATIONAL INTELLIGENCE AND ARTIFICIAL INTELLIGENCE IN GAMES and has been a Guest Editor for several IEEE TRANSACTIONS and journals. He has been serving on several technical program committees of numerous IEEE and ACM events. He has been the General Chair and/or Technical Program Chair of over 20 international conferences, symposia, and workshops on collaborative haptic-audio-visual environments, multimedia communications, and instrumentation and measurement. He was a General Co-Chair of the Association for Computing Machinery (ACM) Multimedia 2008. He is a Senior Member of the ACM, an IEEE Distinguished Lecturer, and a Fellow of the Canadian Academy of Engineering.